Pressure Dependence of the Superconducting Transition Temperature of Magnesium Diboride

M. Monteverde,[1] M. Núñez-Regueiro,[1]* N. Rogado,[2] K. A. Regan,[2] M. A. Hayward,[2] T. He,[2] S. M. Loureiro,[2] R. J. Cava[2]

We studied the pressure and temperature dependence of the electrical resistivity of the superconducting compound magnesium diboride (MgB_2). The superconducting transition temperature decreases monotonically with pressure, being parabolic or linear, depending on samples. The rate of decrease under pressure is higher than in conventional superconductors. We discuss our results in terms of the semimetallic character of the electronic band structure of MgB_2.

For decades, the limit of electron-phonon–driven superconductivity in metals was thought to be ~30 K (*1, 2*) as a consequence of the energies of the phonons involved in the conventional Bardeen-Cooper-Schrieffer (BCS)–Eliashberg formulation of superconductivity, which are of the order of 400 K. The present record holders do not actually challenge this thought: High-temperature superconductivity in cuprates is now considered to be due to other electronic mechanisms (*3*), and the superconducting transition temperature of hole-doped C_{60} (T_c = 52 K) will probably require a different theoretical framework that is adapted to its cluster nature (*4*). The question about the limit of metallic superconductivity is the reason why the recent discovery of superconductivity at ~39 K (*5*) in MgB_2 has generated such excitement in the condensed matter physics world: Does it push the limit of conventional superconductivity, or is the superconductivity based on a different mechanism? Two recent theoretical papers propose opposing scenarios. From band structure calculations, Kortus *et al.* (*6*) affirm that MgB_2 represents the first known case of metallic boron. Because the boron atoms have a light mass, we obtain a metal with very high phonon frequencies, ~700 K. Coupled to a strong electron-phonon interaction, this would indeed yield the observed high T_c. In addition, the isotope effect measurements (*7*) support the apparent conventional BCS nature of superconductivity in MgB_2. On the other hand, the band structure is complex, because both two-dimensional (2D) and three-dimensional (3D) bands originating from p_{xy} and p_z orbitals, respectively, are present at the Fermi level. Hirsch (*8*) remarks that the presence of 2D p_{xy} holes suggests a mechanism analogous to that of superconducting 2D cuprates.

Studies of superconducting materials under pressure are useful for elucidating superconducting behavior as well as for seeking out new phases. A recent example is the discovery of superconductivity (*9, 10*) at ~14 K in the AlB_2 phase of $CaSi_2$, the highest ever obtained in silicides. Also, it is at high pressure that the highest superconducting temperatures have been observed in Hg-1223 (*11–13*). We report the results of resistivity measurements of MgB_2 at pressures up to 25 GPa in order to study the pressure dependence of the superconducting transition and the phase stability of the AlB_2 structure type for this material.

The samples employed were synthesized by direct reaction of the elements. Starting materials were bright magnesium flakes (Aldrich Chemical, Milwaukee, Wisconsin), fine aluminum powder (Alfa Inorganics, Beverly, Massachusetts), and submicrometer amorphous boron powder (Callery Chemical, Evans City, Pennsylvania). Starting materials were mixed in a half-gram batch and sealed in a molybdenum tube under argon. The molybdenum tube was in turn sealed in an evacuated quartz ampoule. The sample was heated for 1 hour at 600°C, 1 hour at 800°C, and 2 hours at 950°C, and then lightly ground. This material provided powder sample 1. The same powder was then hot-pressed at 10 kbar for 1 hour at 700°C to supply ceramic sample 2. The preparation of sample 3 was identical to that of sample 1 but was heated for only 1 hour at 950°C, whereas sample 4 was prepared by using a tantalum tube heated at 900°C for 3 hours.

Four-probe dc electrical resistivity measurements were performed in a sintered diamond Bridgman anvil apparatus, with a pyrophillite gasket and two steatite disks as the pressure medium. The pressure spread across the sintered diamond anvils was previously determined on lead manometers to be ~1.5 to 2 GPa, depending on the applied pressure.

Before cell charging, we performed ac susceptibility characterization of the samples. The powder employed had a very sharp transition measured by ac susceptibility. In sample 1, we observed a maximum onset transition temperature of 38.5 K, with a slight (<0.3 K) splitting of the ac susceptibility χ'' peak, indicating the presence of some small sample inhomogeneity. The sintered sample 2 showed a similar splitting with a higher onset temperature of 39.5 K but a much larger transition width. Sample 3 had several transitions, starting at 38.8 K, whereas sample 4 had only one transition, at 38.6 K

In analyzing the electrical resistivity measurements (Fig. 1), we take into consideration that these measurements have been made on the powder sample and that as very high pressures are being applied, sintering of the powders takes place. The transformation of a poorly connected powder to a sintered powder can alter the temperature dependence of the sample's resistance. In general, the decrease in resistance is due to the better coupling between the sintered grains. We observed a decrease of the resistance with pressure that can, most probably, be attributed to this effect. An increase of carriers or a decrease of the electron-phonon scattering rate may also play a role.

The resistance of sample 1 at low pressures displays metallic behavior at high temperatures, with a minimum at ~150 K (T^* on

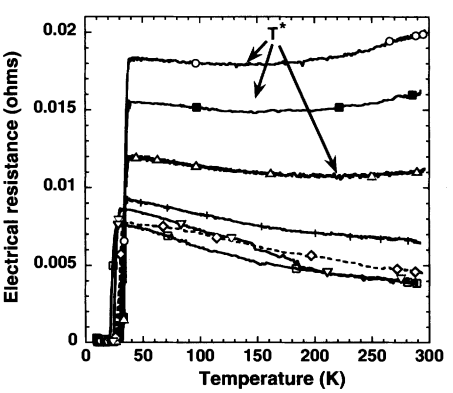

Fig. 1. Temperature dependence of the electrical resistance of MgB_2 powder sample 1 for several pressures. T^* marks the beginning of the upturn in the resistance (open circles, 1.8 GPa; solid squares, 3 GPa; triangles, 6.8 GPa; crosses, 10.5 GPa; diamonds, 14 GPa; inverted triangles, 17 GPa; open squares, 21 GPa).

[1]Centre de Recherches sur les Très Basses Températures, CNRS, BP166 Cedex 09, 38042 Grenoble, France. [2]Department of Chemistry and Materials Institute, Princeton University, Princeton, NJ 08544, USA.

*To whom correspondence should be addressed. E-mail: nunez@polycnrs-gre.fr

Fig. 1), and thermally activated behavior below. As the pressure is increased, the temperature range of the activated regime increases, and above 10 GPa, the metallic dependence of the resistivity is not seen below 300 K. The minimum does not appear to correspond to a distortive phase transition, as the logarithmic derivative of the resistance, normally used to detect electronically driven phase transitions (*14*), does not show any peak or anomaly. The activated behavior also does not appear to be the result of grain boundary scattering: If it were due to the powder nature of the sample, it should become less important with pressure instead of becoming more pronounced. On the other hand, the behavior of mixed metal-insulator powder samples should follow (*15*) the law $\sim\exp[2(C/k_BT)^{-1/2}]$, where C is a constant and k_B is Boltzmann's constant. We did not see this dependence in any temperature region for our sample. All this seems to indicate that the activated behavior of sample 1 is, at least partly, intrinsic.

Looking at the dependence of the superconducting transition with applied pressure (Fig. 2), we found that the width of the transition does not increase with pressure, indicating that the two slightly different T_c values observed in the ac susceptibility vary with the same pressure rate. To obtain the T_c values, we calculated the temperature derivative of the resistance: $T_{c\text{-onset}}$ is the point at which the derivative starts to increase. T_c decreases monotonically with pressure and has a parabolic dependence for samples 1 and 2 and a linear dependence for samples 3 and 4 (Fig. 3). It is instructive to compare our data with those of the highest T_c borocarbide (*16*), $YPd_5B_3C_{0.3}$. The superconducting transition temperature decreases (*17*) in the borocarbide with a rate of 0.29 K/GPa up to 22 GPa (Fig. 3). Although for MgB_2 the slope of the samples with linear dependence is considerably steeper, −0.8 K/GPa, the initial rate (up to ~7 GPa) for the other samples is 0.35 K/GPa and, at higher pressures (P), follows a purely quadratic dependence, $T_c = 38.6\ \text{K} - 0.0263\ \text{K/GPa} \times P^2$. These rates fall within the high range of T_c pressure dependence of superconducting metals (*18*).

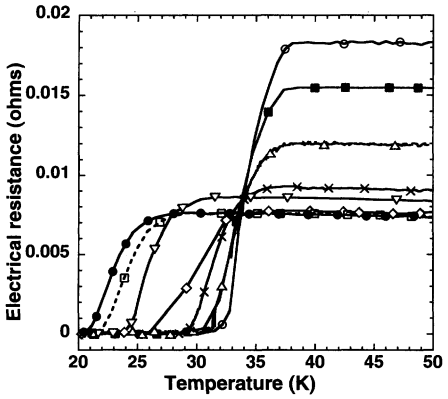

Fig. 2. Detail showing the resistance superconducting transition for several pressures (open circles, 1.8 GPa; solid squares, 3 GPa; triangles, 6.8 GPa; crosses, 10.5 GPa; diamonds, 14 GPa; inverted triangles, 17 GPa; open squares, 19 GPa; solid circles, 21 GPa).

According to the band structure calculations, a dilatation of the lattice (*6*) should increase T_c through an increase of the density of states due to band narrowing. Pressure should have the opposite effect, and thus, the decrease of T_c is in accordance with band calculations. However, the thermally activated behavior of the resistivity under high pressures of samples 1 and 2 cannot be simply explained. A rigid band approach supposing band widening would imply a drifting away from band edge localization effects and a more metallic behavior under pressure. Along these lines, a structural transition under pressure seems more plausible. Because of the layered nature of the AlB_2 structure, we expect an anisotropic compression of the structure. The stiff "graphitic" boron layers should be barely compressible, whereas compression along the c direction should be more facile. As in the case of the hexagonal graphite-diamond transformation, our pressure range may be sufficiently high to allow the interaction between different boron layers and the structural transformation toward another, probably insulating, phase. However, a structural transformation at high pressures cannot explain the low-pressure behavior, unless local distortions of the high-pressure phase are present as defects on the ambient pressure AlB_2 lattice. On the other hand, the vicinity of structural instabilities in phase space is known to favor high transition temperatures within conventional electron-phonon mechanisms (*19*).

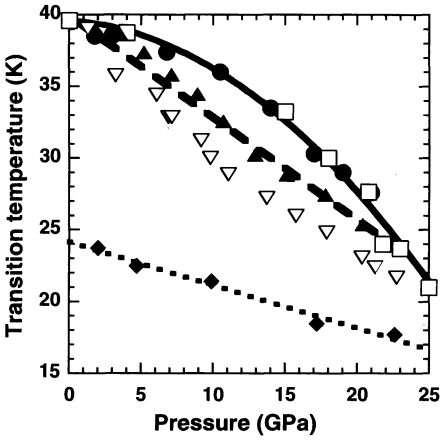

Fig. 3. Pressure dependence of the superconducting transition temperature $T_{c\text{-onset}}$ for MgB_2 (circles, sample 1; squares, sample 2; triangles, sample 3; inverted triangles, sample 4). The pressure dependence for yttrium-palladium-boron-carbon (Y-Pd-B-C) measured in the same apparatus (diamonds) is taken from (*17*). The pressure gradient is 2 GPa, and the transition widths range from 5 to 10 K. The solid line is the purely parabolic fit of the $T_{c\text{-onset}}$ of MgB_2 samples 1 and 2, the dotted line is the linear fit of the $T_{c\text{-onset}}$ of sample 3, and the dashed line is the linear fit of the $T_{c\text{-onset}}$ of the Y-Pd-B-C sample.

The difference behavior of T_c may be attributed to the particular nature of the band structure of MgB_2. Because there are different sets of bands crossing the Fermi level with a semimetallic character (thus yielding three different type of carriers), we can expect a large sensitivity to defects or magnesium nonstoichiometry. The quadratic dependence of T_c with pressure suggests a comparison of MgB_2 to the high-temperature cuprate superconductors (HTSCs) (*20*). It seems as if pressure is changing the carrier concentration in MgB_2 in a manner similar to that observed in HTSCs: In other words, the application of pressure would decrease (increase for HTSCs) the carrier concentration. We can speculate that, as a result of the probable anisotropic compression, the p_z 3D bands will widen at a stronger rate under pressure than will the p_{xy} bands. A gradual transfer of holes from the p_{xy} bands to the p_z band can then gradually occur under pressure. The decrease of T_c with pressure would then be related to the loss of p_{xy} holes under pressure. Within this line of thought, the steeper linear behavior of samples 3 and 4 seems to indicate that these samples have a different degree of doping that is equivalent to a higher starting pressure.

The change from decreasing to increasing behavior of the resistivity at T^* was observed in both sample 1 (Fig. 1) and sample 2 (Fig. 4) but not in samples 3 and 4, which show a metallic behavior at all pressures and temperatures. The unusual behavior may be due to pretransitional behavior, like a pseudogap as in underdoped HTSCs. The pressure depen-

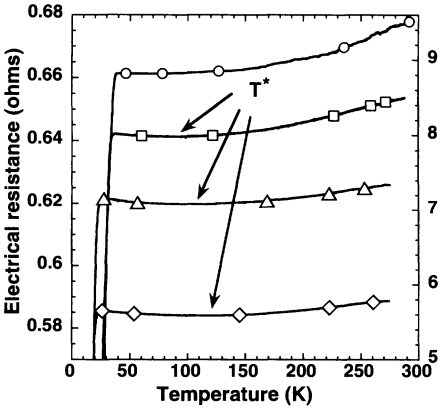

Fig. 4. Temperature dependence of the electrical resistance of the MgB_2 sintered ceramic sample 3 for several pressures. T^* marks the beginning of the upturn in the resistance. For the first pressure (right scale), there is no upturn (circles, 1.8 GPa; squares, 15 GPa; triangles, 25 GPa; diamonds, 26 GPa).

dence, T^* increasing with decreasing T_c, is the expected one for such a pseudogap. But the values of T^* are different for the two samples. Other processes, such as localization by defects, most likely are in play, because in underdoped cuprates the value of the characteristic energy T^* does not change substantially between different samples (*21*).

References and Notes

1. W. L. McMillan, *Phys. Rev.* **167**, 331 (1968).
2. V. L. Ginzburg, D. A. Kirzhnits, Eds., *High Temperature Superconductivity* (Consultants Bureau, New York, 1982).
3. P. W. Anderson, *Science* **288**, 480 (2000).
4. J. H. Schön, Ch. Kloc, B. Batlogg, *Nature* **408**, 549 (2000).
5. J. Akimitsu, paper presented at the Symposium on Transition Metal Oxides, Sendai, Japan, 10 January 2001.
6. J. Kortus, I. I. Mazin , K. D. Belashchenko, V. P. Antropov, L. L. Boyer, e-Print available at http://arXiv.org/abs/cond-mat/0101446.
7. S. L. Bud'ko *et al.*, *Phys. Rev. Lett.* **86**, 1877 (2001) (e-Print available at http://arXiv.org/abs/cond-mat/0101463).
8. J. E. Hirsch, e-Print available at http://arXiv.org/abs/cond-mat/0102115.
9. S. Sanfilippo *et al.*, *Phys. Rev. B* **61**, R3800 (2000).
10. P. Bordet *et al.*, *Phys. Rev. B* **62**, 11392 (2000).
11. C. W. Chu *et al.*, *Nature* **365**, 323 (1993).
12. M. Núñez-Regueiro, J.-L. Tholence, E. V. Antipov, J.-J. Capponi, M. Marezio, *Science* **262**, 97 (1993).
13. L. Gao *et al.*, *Phys. Rev. B* **50**, 4260 (1994).
14. P. M. Horn, C. Guidotti, *Phys. Rev. B* **16**, 491 (1977).
15. B. Abeles, P. Sheng, M. D. Coutts, Y. Arie, *Adv. Phys.* **24**, 407 (1975).
16. R. J. Cava *et al.*, *Nature* **367**, 146 (1994).
17. M. Núñez-Regueiro *et al.*, *Physica C* **235–240**, 2093 (1994).
18. M. Núñez-Regueiro, C. Acha, in *Hg-Based High* T_c *Superconductors*, A. Narlikar, Ed., vol. 24 of *Studies of High Temperature Superconductors* (Nova Science, New York, 1997), pp. 203–240.
19. B. T. Matthias, in *Superconductivity of d- and f-Band Metals* (American Institute of Physics, New York, 1972), p. 367–376.
20. H. Takagi *et al.*, *Phys. Rev. Lett.* **69**, 2975 (1992).
21. D. K. Finnemore, J. E. Ostenson, S. L. Bud'ko, G. Lapertot, P. C. Canfield, e-Print available at http://arXiv.org/abs/cond-mat/0102114.

22. We acknowledge P. Monceau, B. Chakraverty, D. Núñez-Regueiro, C. Paulsen, and J.-L. Tholence for a critical reading of the manuscript and J. Ranninger and B. Batlogg for enlightening discussions. M.M. is a Consejo Nacional de Investigaciones Científicas y Técnicas (Argentina) doctoral fellow.

12 February 2001; accepted 22 February 2001
Published online 8 March 2001;
10.1126/science.1059775
Include this information when citing this paper.

Experimental Verification of a Negative Index of Refraction

R. A. Shelby, D. R. Smith, S. Schultz

We present experimental scattering data at microwave frequencies on a structured metamaterial that exhibits a frequency band where the effective index of refraction (*n*) is negative. The material consists of a two-dimensional array of repeated unit cells of copper strips and split ring resonators on interlocking strips of standard circuit board material. By measuring the scattering angle of the transmitted beam through a prism fabricated from this material, we determine the effective *n*, appropriate to Snell's law. These experiments directly confirm the predictions of Maxwell's equations that *n* is given by the negative square root of $\varepsilon \cdot \mu$ for the frequencies where both the permittivity (ε) and the permeability (μ) are negative. Configurations of geometrical optical designs are now possible that could not be realized by positive index materials.

Refraction is perhaps one of the most basic of electromagnetic phenomena, whereby when a beam of radiation is incident on an interface between two materials at an arbitrary angle, the direction of propagation of the transmitted beam is altered by an amount related to the indices of refraction of the two materials. Snell's law, arrived at by requiring that the phase of the incident and transmitted beams be the same everywhere at the interface, provides the quantitative relation between the incident and refractive angles (θ_1 and θ_2, measured from the refraction interface normal) and the indices of refraction of the media (n_1 and n_2), having the form $n_1 \sin(\theta_1) = n_2 \sin(\theta_2)$. A refracted ray is thus bent toward the normal (but never emerges on the same side of the normal as the incident ray) upon entering a naturally occurring material from air, as most materials have $n > 1$. Refraction forms the basis of lenses and imaging, as any finite section of material with an index differing from that of its environment will alter the direction of incoming rays that are not normal to the interface. Lenses can be designed to focus and steer radiation for a wide variety of applications and are of use over a large range of wavelengths (e.g., from radio to optical).

Although all known naturally occurring materials exhibit positive indices of refraction, the possibility of materials with negative refractive index has been explored theoretically (*1*) and the conclusion presented that such materials did not violate any fundamental physical laws. These materials were termed "left-handed" (LHM), and it was further shown that some of the most fundamental electromagnetic properties of an LHM would be opposite to that of ordinary "right-handed" materials (RHM), resulting in unusual and nonintuitive optics. A beam incident on an LHM from an RHM, for example, refracts to the same side of the normal as the incident ray. Furthermore, it was predicted that the rays from a point source impinging on a flat, parallel slab of LHM would be refocused to a point on the opposite side of the material. Recently, analysis of this situation produced the observation that such a planar slab, if of suitable index, can produce a focus with subwavelength resolution, beating the normal diffraction limit associated with positive refractive index optics (*2*).

The fabrication and measurement of structured metamaterials having a range of frequencies over which the refractive index was predicted to be negative for one direction of propagation were reported recently (*3*). An extension of this structure to two dimensions was subsequently introduced and predicted to exhibit an isotropic, negative index in two dimensions (*4*). These structures use split ring resonators to produce negative magnetic permeability over a particular frequency region (*5*) and wire elements to produce negative electric permittivity in an overlapping frequency region (*6*). When the permittivity, ε, and permeability, μ, of a material are simultaneously negative, one must choose the negative root of the index of refraction given by $n = \pm\sqrt{\varepsilon\mu/\varepsilon_0\mu_0}$ (ε_0 and μ_0 are the free-space permittivity and permeability, respectively) (*1*, *2*, *7*). Although the recent transmission experiments and simulations (*3*, *4*) on LHMs demonstrated the presence of a left-handed propagation band, the experiments presented here directly confirm that LHMs do indeed exhibit negative refraction.

The LHM sample used in the experiments presented here (Fig. 1) consists of a two-dimensionally periodic array of copper split ring resonators and wires, fabricated by a shadow mask/etching technique on 0.25-mm-thick G10 fiber glass circuit board material. After processing, the boards were cut and assembled into an interlocking unit, from which a prism-shaped section was cut for the beam-deflection experiments.

To determine the refractive index, we measured the deflection of a beam of microwave radiation as the beam passed through the prism-shaped sample. In this refraction experiment (Fig. 2), the prism-shaped samples were placed between the two circular

Department of Physics, University of California, San Diego, La Jolla, CA 92093–0350, USA.